Journal of Hazardous Materials 192 (2011) 131–138

Contents lists available at ScienceDirect

Journal of Hazardous Materials

journal homepage: www.elsevier.com/locate/jhazmat

# Arsenic (III,V) removal from aqueous solution by ultrafine α-$Fe_2O_3$ nanoparticles synthesized from solvent thermal method

Wenshu Tang[a], Qi Li[a,*], Shian Gao[a], Jian Ku Shang[a,b]

[a] Materials Center for Water Purification, Shenyang National Laboratory for Materials Science, Institute of Metal Research, Chinese Academy of Sciences, Shenyang, 110016, PR China
[b] Department of Materials Science and Engineering, University of Illinois at Urbana-Champaign, Urbana, IL 61801, USA

ARTICLE INFO

*Article history:*
Received 22 September 2010
Received in revised form 22 March 2011
Accepted 30 April 2011
Available online 23 May 2011

*Keywords:*
Arsenite
Arsenate
Adsorption
Competing anions
α-$Fe_2O_3$ nanoparticles

ABSTRACT

Ultrafine iron oxide (α-$Fe_2O_3$) nanoparticles were synthesized by a solvent thermal process and used to remove arsenic ions from both lab-prepared and natural water samples. The α-$Fe_2O_3$ nanoparticles assumed a near-sphere shape with an average size of about 5 nm. They aggregated into a highly porous structure with a high specific surface area of ~162 $m^2/g$, while their surface was covered by high-affinity hydroxyl groups. The arsenic adsorption experiment results demonstrated that they were effective, especially at low equilibrium arsenic concentrations, in removing both As(III) and As(V) from lab-prepared and natural water samples. Near the neutral pH, the adsorption capacities of the α-$Fe_2O_3$ nanoparticles on As(III) and As(V) from lab-prepared samples were found to be no less than 95 mg/g and 47 mg/g, respectively. In the presence of most competing ions, these α-$Fe_2O_3$ nanoparticles maintained their arsenic adsorption capacity even at very high competing anion concentrations. Without the pre-oxidation and/or the pH adjustment, these α-$Fe_2O_3$ nanoparticles effectively removed both As(III) and As(V) from a contaminated natural lake water sample to meet the USEPA drinking water standard for arsenic.

© 2011 Elsevier B.V. All rights reserved.

## 1. Introduction

Arsenic is well known for its toxicity to human beings [1]. Long-term exposure to arsenic contaminated water causes skin, lung, bladder, and kidney cancer as well as pigmentation changes, skin thickening (hyperkeratosis), neurological disorders, muscular weakness, loss of appetite, and nausea [2]. Arsenic contamination in natural water is a worldwide problem, as reported in the USA, China, Chile, Bangladesh, Mexico, Argentina, Poland, Canada, Hungary, New Zealand, Japan, Vietnam, and India [3–5]. To avoid the adverse health effects of arsenic, the World Health Organization (WHO) suggested that the maximum contaminant level (MCL) for arsenic in drinking water should be lowered from 0.05 to 0.01 mg/L [6]. To implement such a stricter MCL requires the development of simple, cost effective approaches for As removal from drinking water.

Various arsenic removal technologies have been developed for arsenic removal from contaminated water sources, including precipitation, membrane processes, ion exchange, and adsorption [1,3,7]. Because of its simplicity, potential for regeneration, and sludge free operation, adsorption technique is attracting more and more attentions [1,8]. In natural water environment, arsenic is mostly found in inorganic form as oxyanions of trivalent (As(III)) or pentavalent arsenic (As(V)) [9]. It is generally reported that As(III) does not have a high affinity to the surface of various adsorbents compared to As(V) because As(III) exists mainly as non-ionic $H_3AsO_3$ at pH values ranging from weakly acidic to weakly alkaline [10], even though As(III) is more mobile and toxic in biological systems than As(V). Thus, a pre-treatment of As(III) by oxidizing it to As(V) and/or adjusting the pH value of water before coagulation–precipitation or adsorption processes is necessary and recommended for the effective removal of As(III) from water [11,12]. However, for the treatment of large natural water bodies contaminated with As(III), it is difficult or even impossible to conduct such a pre-treatment and after-treatment pH adjustment. Thus, it is desirable to develop adsorbents with a good adsorption effect on both As(III) and As(V) without pre-treatment [13].

Because of their low cost and affinity to arsenic, various iron oxides, including amorphous hydrous ferric oxide (FeOOH), goethite (α-FeOOH), and hematite (α-$Fe_2O_3$), have been extensively studied in various forms for the removal of arsenic from water [14–29]. Although the amorphous FeOOH and goethite have the high surface areas, which are deemed beneficial to the adsorption process, they are not stable and could easily decompose or form low surface-area crystalline iron oxides during the synthesis and usage, which will greatly reduce their As removal capacity [18]. α-$Fe_2O_3$, however, has a high stability, which may have great potential for the removal of arsenic [7]. Till now, most reports on

* Corresponding author. Tel.: +86 24 83978028; fax: +86 24 23971703.
*E-mail address:* qili@imr.ac.cn (Q. Li).

0304-3894/$ – see front matter © 2011 Elsevier B.V. All rights reserved.
doi:10.1016/j.jhazmat.2011.04.111

the arsenic removal by α-$Fe_2O_3$ are concentrated on using natural hematite [7,14,20–26]. Reports are limited for the use of synthetic nano-sized α-$Fe_2O_3$ to remove arsenic (most on As(V)) [27–29], and no systematic study had been made on the removal of As(III) from water with nano-sized α-$Fe_2O_3$.

In this study, ultrafine α-$Fe_2O_3$ nanoparticles were synthesized by the solvent thermal process and their adsorption effect on As(III) and As(V) were investigated in both lab-prepared and natural water samples at near neutral pH environment. Partly becauae of the large surface areas, these ultrafine α-$Fe_2O_3$ nanoparticles demonstrated a strong adsorption of both As(III) and As(V) in lab-prepared water samples, especially when the arsenic contamination concentration was low. The strong arsenic adsorption was not greatly affected by the presence of competing anions. Consequently, these α-$Fe_2O_3$ nanoparticles successfully removed most of the As(III) and As(V) contamination from natural water samples of Lake Yangzonghai, which included multiple competing ions such as $Cl^-$, $SO_4^{-2}$, and $F^-$, to meet the USEPA standard for arsenic in drinking water. With further development, this technology may offer a simple single-step treatment option to treat arsenic contaminated natural water without the pretreatment as required of the current industrial practice.

## 2. Experimental

### 2.1. Chemicals and materials

All the reagents are of analytical grade and used as received. Ferric chloride anhydrous ($FeCl_3$, 99.0 wt%, Chemical Reagent Co. Ltd., Beijing, PR China) served as the iron source in the solvent thermal process. Ethanol ($C_2H_5OH$, ≥99.0 wt%, Yili Chemical Reagent Co. Ltd., Beijing, PR China) was the solvent. Sodium hydroxide (NaOH, 98 wt%, Tianjin Damao Chemical Reagents Development Center, Tianjin, PR China) was chosen to be the precipitation agent. As(III) and As(V) stock solutions (~200 mg/L) were prepared by dissolving sodium arsenite ($NaAsO_2$, 99.0 wt%, Shanghai Tian Ji Chemical Institute, Shanghai, PR China) and sodium arsenate ($Na_3AsO_4$, 99.0 wt%, Shanghai Tian Ji Chemical Institute, Shanghai, PR China) into deionized water, respectively, and stored in the dark in a refrigerator at 4 °C. For the study on the effect of competing coexisting anions on arsenic adsorption, the stock solutions (1 M) of NaF, NaCl, $NaNO_3$, $Na_2SO_4$, $NaHCO_3$, $Na_2HPO_4{\cdot}12H_2O$, and $Na_2SiO_3{\cdot}9H_2O$ (≥99.0 wt%, Shenyang Guo Yao Technology, Shenyang, China) were prepared by dissolving the respective chemicals in deionized water. Concentrated hydrochloric acid (HCl, 32–38%, Tianda Chemical Reagents Factory, Tianjin, PR China) was used to stabilize the arsenic species after treatment. For comparison, a commercially available α-$Fe_2O_3$ powder (98%, average size ~ 100 nm, specific surface area ~ 11.2 $m^2$/g, the Shenyi Chemical Reagent Co. Ltd., Shenyang, PR China) was evaluated for arsenic adsorption against the ultrafine α-$Fe_2O_3$ nanoparticles synthesized in this study.

### 2.2. Preparation of ultrafine α-$Fe_2O_3$ nanoparticles

In a typical process, the synthesis involved three steps. First, a solution of $FeCl_3$ at a concentration of 0.1 M was obtained by dissolving 1.13 g anhydrous $FeCl_3$ into 80 mL ethanol in a beaker. 0.8 g NaOH was then added into the $FeCl_3$ solution. After 1 h of the reaction between $FeCl_3$ and NaOH at room temperature under constant magnetic stirring, a precursor solution was obtained in the form of a yellow-brown suspension. Next, the precursor solution was transferred into a 100 mL Teflon-lined autoclave. The autoclave was then placed in an oven preheated to150 °C and kept in the oven for 2 h before the oven was cooled to room temperature naturally. Finally, the red precipitation in the autoclave was washed three times using distilled water to remove NaCl, once using alcohol, and then dried at 80 °C for 12 h to obtain ultrafine α-$Fe_2O_3$ nanoparticles.

### 2.3. Characterization of ultrafine α-$Fe_2O_3$ nanoparticles

The crystal structure of α-$Fe_2O_3$ nanoparticles was analyzed by X-ray diffraction (XRD) on a D/MAX-2004 X-ray powder diffractometer (Rigaku Corporation, Tokyo, Japan) with Ni-filtered Cu Kα ($\lambda$ = 1.54178 Å) radiation at 56 kV and 182 mA. The $2\theta$ range used in the measurement was from 20° to 80°. Transmission electron microscopy (TEM) was used for the morphology observation of α-$Fe_2O_3$ nanoparticles on a JEM 2100 transmission electron microscope (JEOL Corporation, Tokyo, Japan) operated at 200 kV. TEM sample was made by dispersing α-$Fe_2O_3$ nanoparticles in ethanol, applying a drop of the dispersion on a Cu grid, and drying in air. Brunauer–Emmett–Teller (BET) surface area and the pore-size distribution (PSD) of α-$Fe_2O_3$ nanoparticles were measured by $N_2$ adsorption–desorption isotherm with an Autosorb-1 Series Surface Area and Pore Size Analyzers (Quantachrome Instruments, Boynton Beach, FL, U.S.A.). Prior to the experiments, samples were dehydrated at 130 °C for 12 h. The relative pressure ($P/P_0$) of 0.1018–0.3056 was used to determine the BET surface area. The pore-size distribution (PSD) was calculated using the desorption branches of the $N_2$ adsorption isotherm and the Barrett–Joyner–Halenda (BJH) formula [30]. The average pore diameter was obtained from the PSD curves. The IR–vis spectra of α-$Fe_2O_3$ nanoparticles were measured at room temperature in transmission mode by the Fourier transform infrared spectroscopy (FTIR, Bruker TENSOR 27, MCT detector) with a resolution of 4 $cm^{-1}$. Samples for FTIR observation were ground with spectral grade KBr in an agate mortar.

### 2.4. Batch arsenic adsorption experiments

All the experiments of arsenic adsorption were carried out at ~25 °C. During the arsenic removal experiment, the arsenic solutions were stirred magnetically to disperse α-$Fe_2O_3$ nanoparticles to ensure a good contact with arsenic contaminations. After recovering the adsorbent by centrifugation at $10^4$ rpm for 30 min, one drop of concentrated HCl was added into the clear solution to avoid the potential oxidation of As(III) to As(V). The As(III) and As(V) concentrations of the aqueous solutions were determined by an atomic fluorescence spectrophotometer (AFS-9800, Beijing Ke Chuang Hai Guang Instrument Inc., Beijing, PR China) with the valence analysis function. Detailed information on experiment conditions could be found in the Supplementary Information.

## 3. Results and discussion

### 3.1. Crystal structure and morphology of α-$Fe_2O_3$ nanoparticles

Fig. 1a shows the XRD pattern of α-$Fe_2O_3$ nanoparticles synthesized by the solvent thermal process at 150 °C, in which all diffraction peaks are in good agreement with rhomb-centered hexagonal (rch) α-$Fe_2O_3$ ($a$ = 5.035 Å, $c$ = 13.74 Å, JCPDS Card No. 03-0664). No other peaks were observed, indicating that the as-synthesized sample consists of high-purity, well-crystallized α-$Fe_2O_3$ nanoparticles. This observation demonstrates that the solvent thermal process used here is conducive to the decomposition of $Fe(OH)_3$ and the crystallization of α-$Fe_2O_3$. The solid reaction to produce α-$Fe_2O_3$ nanoparticles usually requires a heat treatment at an elevated temperature, e.g., at ~400 °C, for the phase transition from $Fe(OH)_3$ to α-$Fe_2O_3$ [31]. Thus, the production cost could be reduced with this solvent thermal process due to the elimination of the heat treatment, allowing for an energy-efficient way to synthesize ultrafine nanoparticles.

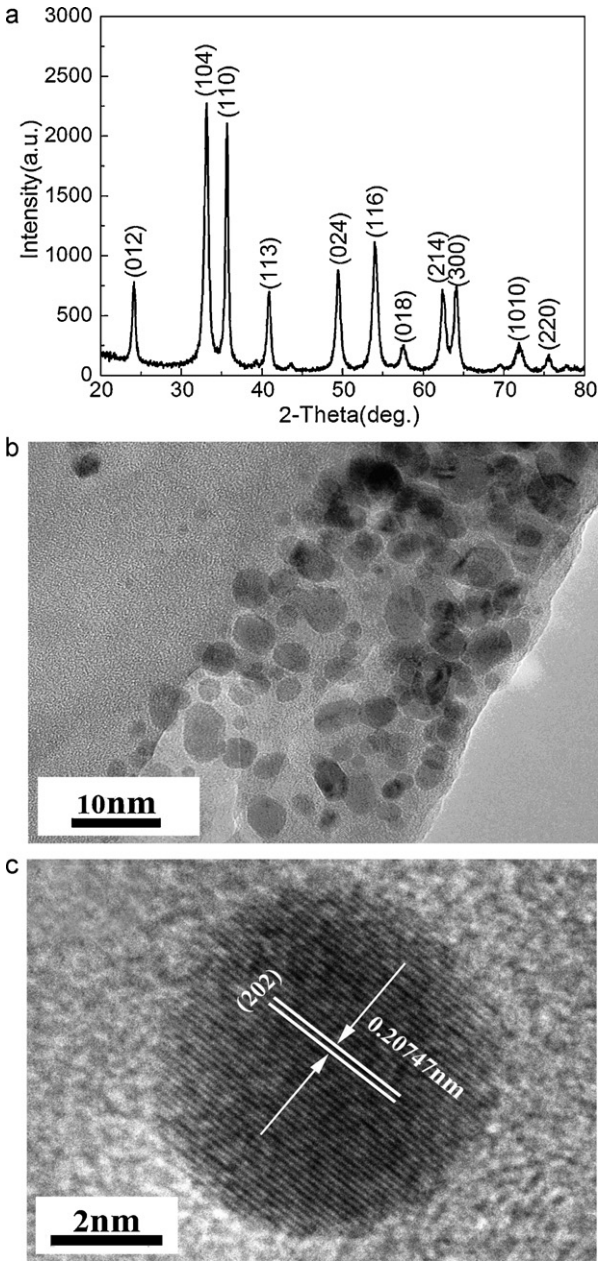


**Fig. 1.** (a) X-ray diffraction pattern, (b) TEM image, and (c) HRTEM image of α-$Fe_2O_3$ nanoparticles.

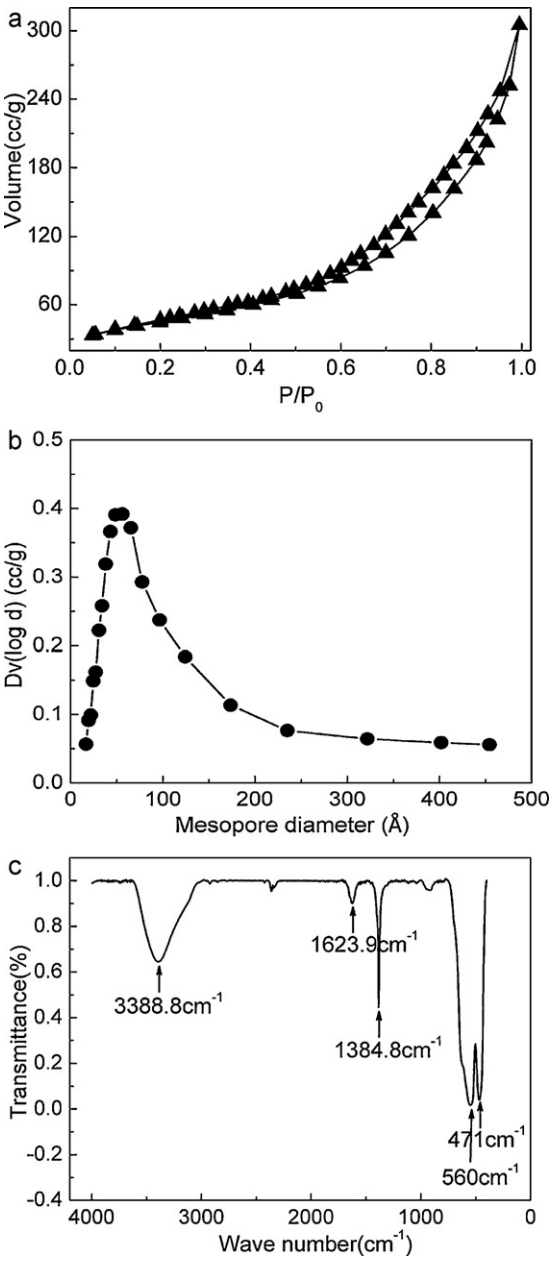


**Fig. 2.** (a) BET curve, (b) Mesopore size distribution, and (c) IR spectra of α-$Fe_2O_3$ nanoparticles.

Fig. 1b shows the TEM image of the final product after washing and drying. After washing with distilled water and ethanol, ultrafine and dispersed α-$Fe_2O_3$ nanoparticles were obtained which had a narrow size distribution of ~3 to 8 nm. Fig. 1c shows the high resolution TEM (HRTEM) image of one ultrafine α-$Fe_2O_3$ nanoparticle, which demonstrates that these nanoparticles have a high degree of crystallinity. A set of lattice planes with the *d*-spacing of ~0.2074 nm could be easily identified, which corresponds to the (2 0 2) plane of hexagonal α-$Fe_2O_3$ phase. This observation suggests that these near-spherical nanoparticles are composed of single hematite crystals.

### 3.2. Surface properties of ultrafine α-$Fe_2O_3$ nanoparticles

The $N_2$ adsorption/desorption isotherms of ultrafine α-$Fe_2O_3$ nanoparticles are shown in Fig. 2a, where adsorption followed the lower curve and the desorption followed the upper curve. From the isotherms, the BET specific surface area of the nanoparticles was calculated to be ~162 $m^2$/g, corresponding to an average particle diameter of 7.0 nm. The shape of the BET curve suggests that there is not much micro-porosity in these α-$Fe_2O_3$ nanoparticles. Fig. 2b shows the pore size distribution of these nanoparticles. Most pores were mesoporous with an average pore diameter of ~5.6 nm, which should reflect the inter-particle porosity in the α-$Fe_2O_3$ nanoparticle aggregates. The total pore volume was determined to be 0.3877 $cm^3$/g. Thus, these α-$Fe_2O_3$ nanoparticles created by the solvent thermal process have a relatively large surface area and pore volume, which is desirable for adsorption.

Fig. 2c shows the FTIR spectra of the α-$Fe_2O_3$ nanoparticles. Two strong adsorption bands at ~560 and 471 $cm^{-1}$ were observed, which are the characteristic of crystalline α-$Fe_2O_3$ phase. A strong adsorption peak was founded at 1384 $cm^{-1}$, which represents the vibration frequency of the coordinated hydroxyl groups. At 1623.9 $cm^{-1}$, there was also a strong adsorption peak for

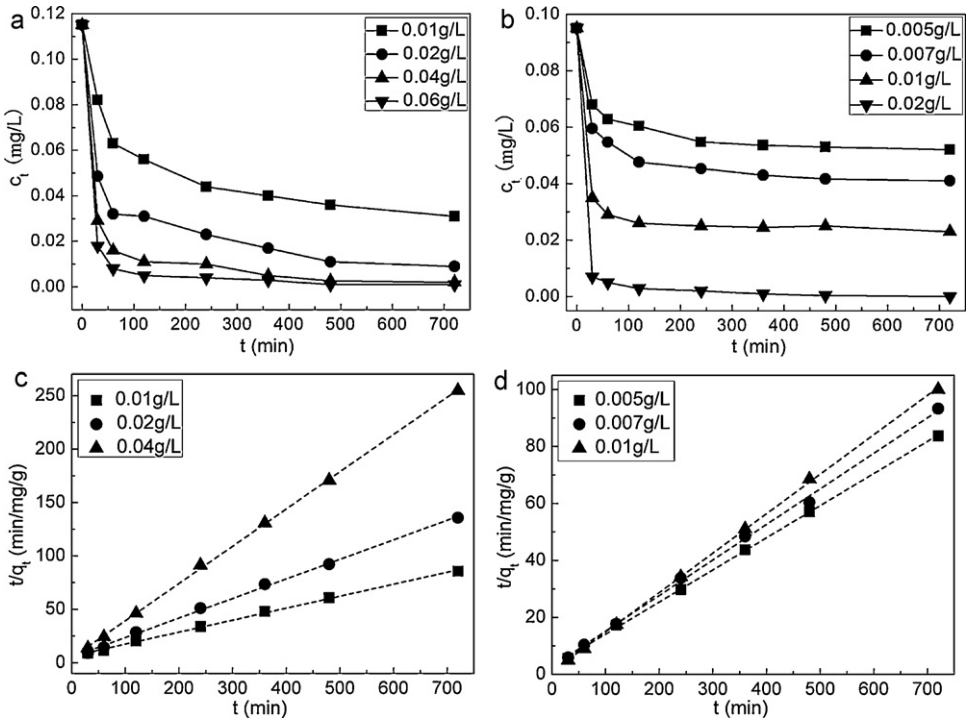


**Fig. 3.** Adsorption kinetics of arsenic in lab-prepared water samples on α-$Fe_2O_3$ nanoparticles: (a) with initial As(III) concentration of ~0.115 mg/L, (b) with initial As(V) concentartion of ~0.095 mg/L.

hydroxyl bending vibration belonging to physically adsorbed $H_2O$. At 3388.8 $cm^{-1}$, the hydroxyl stretching vibration frequency could be found. [32,33]. These observations demonstrate that the α-$Fe_2O_3$ nanoparticles have high adsorption capacities to $H_2O$ and hydroxyl groups exist on their surfaces. The combination of a large surface area and the existence of surface hydroxyl groups on these α-$Fe_2O_3$ nanoparticles should result in strong arsenic adsorption from water.

### 3.3. Kinetic studies on As(III) and As(V) adsorption by α-$Fe_2O_3$ nanoparticles

The kinetics of As(III) and As(V) adsorption at different α-$Fe_2O_3$ nanoparticle loadings in the lab-prepared water samples are shown in Fig. 3. Most of As(III) and As(V) were removed from the contaminated water samples in a short time, before the arsenic concentrations gradually approached a plateau. With the increase of α-$Fe_2O_3$ nanoparticle loading, the removal rate increases and the final equilibrium arsenic concentration in the treated water samples decreases. Fig. 3a shows the variation of the As(III) concentration with time at an initial As(III) concentration of ~0.115 mg/L. It demonstrates that the removal of As(III) by α-$Fe_2O_3$ nanoparticles occurred very rapidly. For example, around 74% As(III) was adsorbed in just 30 min when the α-$Fe_2O_3$ nanoparticle loading concentration was merely 0.04 g/L. The final equilibrium As(III) concentration was about 0.002 mg/L after the treatment, which is far below the USEPA limit for arsenic in drinking water. When the α-$Fe_2O_3$ loading was slightly raised to 0.06 g/L, the equilibrium As(III) concentration could be lowered to zero (less than the instrument detection limit of $1 \times 10^{-4}$ mg/L), representing a 100% removal. Fig. 3b shows the variation of the As(V) concentration with time at an initial As(V) concentration of ~0.095 mg/L. Similarly, α-$Fe_2O_3$ nanoparticles demonstrated a strong adsorption effect for As(V). When the α-$Fe_2O_3$ loading was only 0.02 g/L, the final equilibrium As(V) concentration could be lowered to zero, representing a 100% removal. Thus, a single step arsenic removal process is possible with these α-$Fe_2O_3$ nanoparticles, without pretreatment (oxidation and pH adjustment) and post-treatment pH adjustment.

The above kinetic experimental results could be best fitted into a pseudo-second-order rate kinetic model developed by Ho [34] with the data analysis and graphing software OriginPro 8 (OriginLab Corporation, Northampton, MA, U.S.A.). This observation is similar to the result reported by Meng and co-workers [35]. The integrated pseudo-second-order rate expression [36] is given in Eq. (1):

$$\frac{t}{q_t} = \frac{t}{q_e} + \frac{1}{\left(K_{ad} q_e^2\right)} \quad (1)$$

where $q_e$ and $q_t$ are the amount (mg/g) of arsenic adsorbed at equilibrium and at time $t$, respectively, and $K_{ad}$ is the rate constant of adsorption (mg/(g min)). The kinetics parameters obtained in fitting the experimental data are summarized in Table 1. The

**Table 1**
Kinetics parameters for As(III) and As(V) adsorption onto α-$Fe_2O_3$ nanoparticles.

| Initial As concentration (mg/L) | As(III) | | | | As(V) | | | |
|---|---|---|---|---|---|---|---|---|
| | 0.115 | | | | 0.095 | | | |
| Materials Loading (g/L) | 0.01 | 0.02 | 0.04 | 0.06 | 0.005 | 0.007 | 0.01 | 0.02 |
| $q_e$ (mg/g) | 8.92 | 5.46 | 2.86 | 1.92 | 8.87 | 8.01 | 7.12 | 4.78 |
| $K_{ad}$ (mg/(g min)) | 0.002 | 0.006 | 0.027 | 0.086 | 0.004 | 0.006 | 0.019 | 0.033 |
| $h = K_{ad} q_e^2$ (mg/(g min)) | 0.159 | 0.179 | 0.221 | 0.317 | 0.315 | 0.385 | 0.963 | 0.754 |
| $r^2$ | 0.999 | 0.998 | 0.999 | 0.999 | 0.999 | 0.998 | 0.999 | 0.999 |

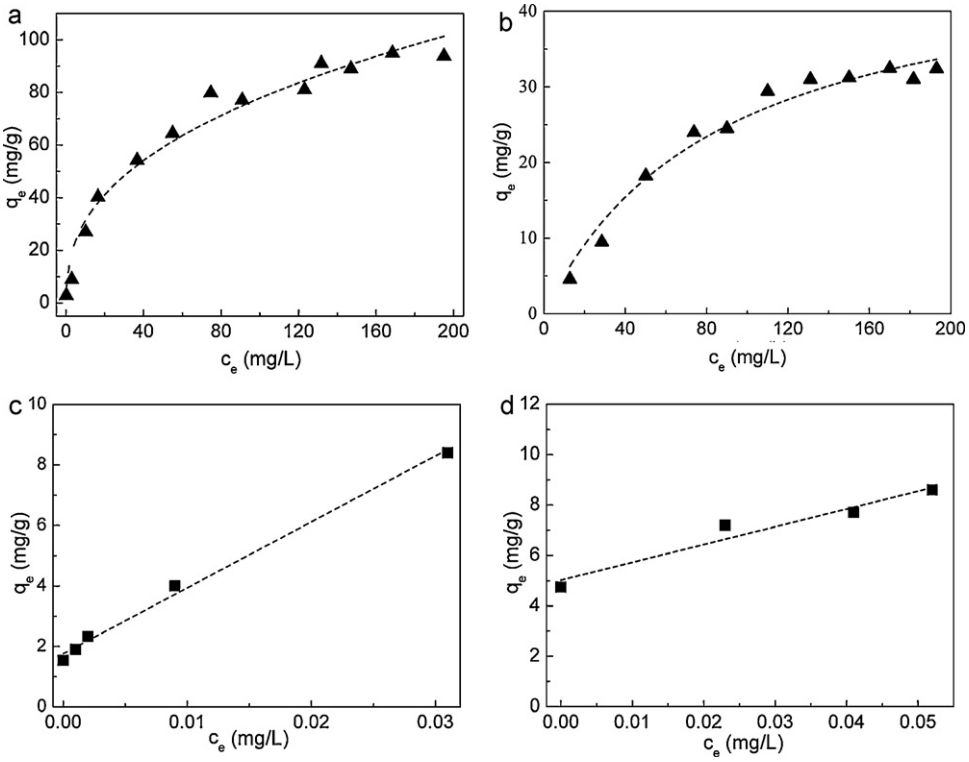


**Fig. 4.** The equilibrium adsorption isotherm of arsenic on α-$Fe_2O_3$ nanoparticles: (a) the equilibrium As(III) concentration was high (up to 200 mg/L), (b) the equilibrium As(V) concentration was high (up to 200 mg/L), (c) the equilibrium As(III) concentration was low (up to 0.03 mg/L), and (d) the equilibrium As(V) concentration was low (up to 0.05 mg/L).

adsorption data for As(III) at an α-$Fe_2O_3$ loading of 0.06 g/L and for As(V) at an α-$Fe_2O_3$ loading of 0.02 g/L were not used in the fitting because all arsenic species were removed and the $q_e$ value could not be determined. Fig. 3c and d demonstrate that the experimental data could be well fitted with the linear form of the pseudo-second order model. The closeness of the square of the correlation coefficients $r$ ($r^2$) to 1 indicates that this kinetic model fitted the experimental data accurately. The initial adsorption rate $h$ ($K_{ad}q_e^2$, mg/(g min)) could be used an indicator of the adsorption rate, especially at the beginning of the adsorption process. It is clear that $h$ increases steadily with the increase of the adsorbent loading for both arsenic species. From Table 1, it is evident that at low arsenic concentrations, the initial adsorption rate of As(V) on α-$Fe_2O_3$ nanoparticles is higher than that of As(III) under the similar experimental conditions, indicating that these α-$Fe_2O_3$ nanoparticles remove As(V) faster than As(III). Similar results were observed for the adsorption of As(III) and As(V) onto ferrihydrite surface [37].

### 3.4. Equilibrium adsorption isotherm studies on As(III) and As(V) adsorption by α-$Fe_2O_3$ nanoparticles

The adsorption capacities of α-$Fe_2O_3$ nanoparticles for As(III) and As(V) near the neutral pH environment were investigated by the equilibrium adsorption isotherm study as demonstrated in Fig. 4; the parameters obtained in fitting the experimental data (with OriginPro 8) are summarized in Table 2. Fig. 4a demonstrates the As(III) equilibrium adsorption isotherm. The As(III) adsorption data could be best fitted with the Freundlich isotherm as given in Eq. (2):

$$q_e = K_F c_e^{1/n} \tag{2}$$

where $q_e$ is the amount (mg/g) of As(III) adsorbed at equilibrium, $c_e$ is the equilibrium As(III) concentration (mg/L) in water samples, and $K_F$ and $n$ are the Freundlich constants of adsorption.

The adsorption capacity of the α-$Fe_2O_3$ nanoparticles synthesized in this study for As(III) did not reach the adsorption saturation even when the equilibrium As(III) concentration reached 200 mg/L. It could further increase with the increase of the equilibrium As(III) concentration. The experiment result here shows that the adsorption capacity of these α-$Fe_2O_3$ nanoparticles for As(III) at the near neutral pH environment should be larger than 95 mg/g. Fig. 4b demonstrates the As(V) equilibrium adsorption isotherm. The As(V) adsorption data could be best fitted with the Langmuir isotherm as given in Eq. (3):

$$q_e = \frac{q_m K_L c_e}{(1/K_L c_e)} \tag{3}$$

**Table 2**
Equlibrium adsorption isotherm fitting parameters for As(III) and As(V) onto α-$Fe_2O_3$ nanoparticles.

| Equilibrium arsenic concentration upper limit (mg/L) | As(III) | | | | As(V) | | | |
|---|---|---|---|---|---|---|---|---|
| | 0.03 | | 200 | | 0.05 | | 200 | |
| | Linear | | Freundlich | | Linear | | Langmuir | |
| Fitting isotherm | $K$ | 216 | $K_F$ | 12.55 | $K$ | 70.56 | $q_m$ | 46.8 |
| | $r^2$ | 0.993 | $r^2$ | 0.970 | $r^2$ | 0.992 | $r^2$ | 0.970 |
| | $b$ | 1.77 | $n$ | 2.53 | $b$ | 5.02 | $K_L$ | 0.011 |

where $q_e$ is the amount (mg/g) of As(V) adsorbed at equilibrium, $q_m$ is the maximum As(V) adsorption capability amount (mg/g), $c_e$ is the equilibrium As(V) concentration (mg/L) in water samples, and $K_L$ is the Langmuir constant of adsorption. The maximum As(V) adsorption capability was determined at ~47 mg/g at pH ~7.

Due to its acute toxic nature, the MCL for arsenic in drinking water was recently lowered to 0.01 mg/L. Thus, the amount of arsenic that an adsorbent could adsorb at low equilibrium concentrations is more important than its maximum adsorption capability in estimating its performance for arsenic removal applications. Fig. 4c and d demonstrates the equilibrium adsorption isotherms under the neutral pH condition at low equilibrium arsenic concentrations for As(III) and As(V), respectively. Under such conditions, the amounts of As(III) and As(V) adsorbed at equilibrium increase by a linear relationship with the increase of the equilibrium arsenic concentration, as described by Eq. (4):

$$q_e = K\, c_e + b \quad (4)$$

where $q_e$ is the amount (mg/g) of arsenic adsorbed at equilibrium, $c_e$ is the equilibrium arsenic concentration (mg/L) in water samples, $K$ (L/g) and $b$ are the adsorption constants. At an equilibrium arsenic concentration of 0.01 mg/L (the standard for drinking water), the amounts of adsorbed As(III) and As(V) were around 4 mg/g and 6 mg/g, respectively. Due to the higher specific surface area, the superior arsenic adsorption capacities of these α-$Fe_2O_3$ nanoparticles at such low equilibrium arsenic concentrations is comparable to or even better than the reported adsorption capacities of various iron oxides at much higher arsenic equilibrium concentrations (over several hundreds of times at tens of ppm).

When the arsenic equilibrium concentration was less than 0.03 mg/L, the amount of As(V) adsorbed at equilibrium was more than the amount of As(III) adsorbed at equilibrium by these α-$Fe_2O_3$ nanoparticles, but it was less than the amount of As(III) adsorbed at equilibrium when the equilibrium arsenic concentration was more than 0.03 mg/L. This observation may be attributed to the different surface charge conditions of As(III) and As(V) species under the neutral pH environment. As(III) exists predominantly as non-charged $H_3AsO_3$ when pH is less than 9.2, while the predominant As(V) species exist as negatively charged $H_2AsO_4^-$ or $HAsO_2^{2-}$ in the pH range from 2.2 to 11.5 [38]. At the neutral pH environment, the surface of α-$Fe_2O_3$ nanoparticles is negatively charged (the isoelectric point or, IEP, at pH 4.9). There should be little repulsive interaction between the nanoparticle and the non-charged As(III) so that the adsorption of As(III) should continue to increase with the As(III) concentration until all the active adsorption sites are occupied. However, for As(V), the negatively charged α-$Fe_2O_3$ nanoparticle surface exerts a coulomb repulsive force to the negatively charged As(V) species, and the adsorbed As(V) species should also have a repulsive effect on As(V) species still in the solution. Therefore, with the increase of the equilibrium arsenic concentration, the amount of As(III) adsorbed at equilibrium would exceed the amount of As(V) adsorbed at equilibrium after a critical equilibrium concentration, as observed experimentally.

### 3.5. As(III) and As(V) adsorption comparison with commercial α-$Fe_2O_3$ powders

To demonstrate the superior arsenic removal effect of the α-$Fe_2O_3$ nanoparticles synthesized in this study, they were compared to a commercial α-$Fe_2O_3$ powders. Fig. 5a demonstrates the As(III) removal percentage in water samples at two different initial As(III) concentrations after the treatment by the two adsorbents. When the initial As(III) concentrations was 1.421 mg/L and the material loading was 0.1 g/L, the α-$Fe_2O_3$ nanoparticles synthesized in this study could remove 87% As(III) in the water sample, while the commercial α-$Fe_2O_3$ powders could remove only 31% As(III) in the water sample. For the lower initial As(III) concentration of 0.078 mg/L at a lower material loading of 0.01 g/L, about 94% As(III) was removed by the newly synthesized α-$Fe_2O_3$ nanoparticles and the remaining As(III) concentration was less than 0.01 mg/L, while the commercial α-$Fe_2O_3$ powders could remove only 18% As(III) under the same experiment conditions. Similar results were observed for As(V) removal. Fig. 5b demonstrates that the newly synthesized α-$Fe_2O_3$ nanoparticles could remove more than twice of the As(V) removed by the commercial α-$Fe_2O_3$ powders. Thus, it is clear that the new α-$Fe_2O_3$ nanoparticles are superior in the removal of arsenic from contaminated water samples because of their higher specific surface area, to the commercial α-$Fe_2O_3$ powders.

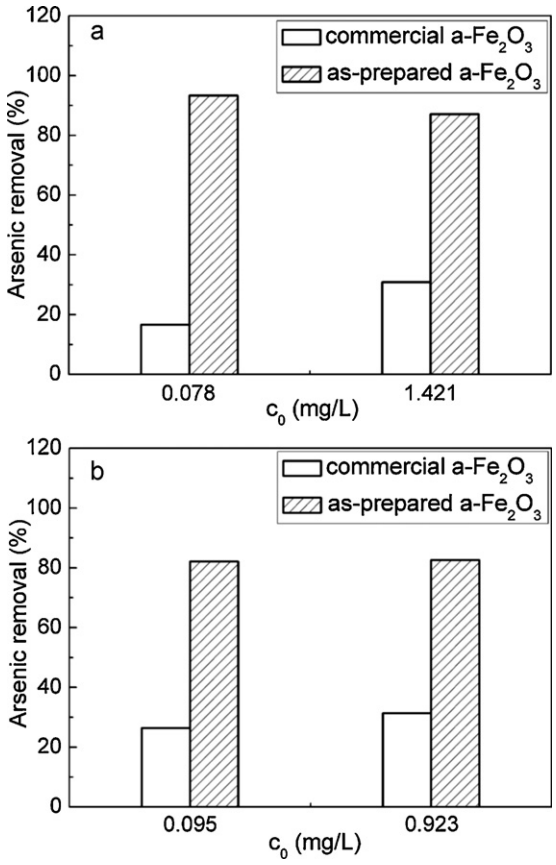


**Fig. 5.** Comparisons of As(III) and As(V) adsorption kinetics between our α-$Fe_2O_3$ nanoparticles and commercial α-$Fe_2O_3$ powder: (a) with initial As(III) concentrations of ~0.078 mg/L and ~1.421 mg/L, respectively; (b) with initial As(V) concentrations of ~0.095 mg/L and ~0.923 mg/L, respectively.

### 3.6. Effect of competing anions on the As(III) and As(V) adsorption

The existence of various ions in natural water may present potential competitions to arsenic adsorption, which may greatly degrade the arsenic removal performance by adsorption on ferric oxide [39,40]. The most abundant competing anions present in natural water are fluoride ($F^-$), chloride ($Cl^-$), nitrate ($NO_3^-$), sulfate ($SO_4^{2-}$), carbonate ($HCO_3^-$), phosphate ($HPO_4^{2-}$) and silica ($SiO_3^{2-}$) [41]. Accordingly, the effects of those competing anions, including $F^-$, $Cl^-$, $NO_3^-$, $SO_4^{2-}$, $HCO_3^-$, $HPO_4^{2-}$ and $SiO_3^{2-}$, on arsenic adsorption by the α-$Fe_2O_3$ nanoparticles were studied as functions of the competing ion concentrations. The material loading of α-$Fe_2O_3$ nanoparticles was fixed at 0.05 g/L, and the results are summarized in Table 3. The presence of $Cl^-$, $NO_3^-$, and $SO_4^{2-}$, even at very high concentrations (100 mM), showed no or just a slight

**Table 3**
Effect of competing anions for As(III) and As(V) onto $\alpha$-$Fe_2O_3$ nanoparticles (note, the removal effect was set as 100% without competing anions).

| Form of As | Competing anion concentration (mM) | % As removed in the presence of: | | | | | | |
|---|---|---|---|---|---|---|---|---|
| | | $F^-$ | $Cl^-$ | $NO_3^-$ | $SO_4^{2-}$ | $HCO_3^-$ | $HPO_4^{2-}$ | $SiO_3^{2-}$ |
| As(III) | 0 | 100 | 100 | 100 | 100 | 100 | 100 | 100 |
| | 10 | 93.2 | 95.1 | 93.8 | 95.8 | 91.9 | 58.0 | 94.4 |
| | 100 | 88.9 | 98.0 | 97.2 | 93.5 | 83.4 | 37.0 | 52.7 |
| As(V) | 0 | 100 | 100 | 100 | 100 | 100 | 100 | 100 |
| | 10 | 71.4 | 99.4 | 100 | 91.8 | 75.5 | 12.4 | 33.3 |
| | 100 | 33.7 | 100 | 98.0 | 77.6 | 63.3 | 5.5 | 18.2 |

**Table 4**
Water quality data of Yangzonghai Lake water.

| Component | Concentration (mg/L) |
|---|---|
| $F^-$ | 0.54 |
| $Cl^-$ | 5.77 |
| $NO_3^-$ | 1.08 |
| $SO_4^{2-}$ | 121.91 |
| $HCO_3^-$ | 89 |
| Total P | 0.061 |
| Na | 170 |
| K | 5 |
| Ca | 24 |
| Mg | 29 |

deterioration effect on the adsorption of both As(III) and As(V) on the $\alpha$-$Fe_2O_3$ nanoparticles, while $H_2PO_4^-$ and $SiO_3^{2-}$ could significantly decrease their arsenic adsorption (especially to As(V) when their concentrations were high). This result is consistent with the observation of Jeong et al. [42]. The concentrations of competing anions used in this study are much higher than arsenic concentration (from over 560 times to 5600 times). The results demonstrate that the $\alpha$-$Fe_2O_3$ nanoparticles are able to remove arsenic species even in the presence of exceptionally high concentrations of competing anions used in this study.

### 3.7. As(III) and As(V) removal in natural water samples by $\alpha$-$Fe_2O_3$ nanoparticles

To examine the removal effect of the $\alpha$-$Fe_2O_3$ nanoparticles on As(III) and As(V) in the natural water environment, arsenic adsorption studies were conducted with the natural water samples from Lake Yangzonghai in the Yunnan Province of China, which was recently contaminated by industrial arsenic pollutions. The contamination was found in over 600 million tons of the lake water, leaving tens of thousands of people living around the lake without access to the lake water for drinking and irrigation. Water quality analysis of the lake water (shown on the Table 4) indicates that besides arsenic, fluoride, chloride, nitrate, sulfate, phosphate, carbonate, and sodium ions were the primary impurities. Fig. 6 demonstrated that the $\alpha$-$Fe_2O_3$ nanoparticles could effectively remove both As(III) and As(V) simultaneously from this natural water sample, in which the As(III) and As(V) concentrations were found at ~0.044 mg/L and ~0.071 mg/L, respectively. Only with a low material loading of 0.1 g/L (0.01 wt%), about 98% As(III) and 96% As(V) were removed by the $\alpha$-$Fe_2O_3$ nanoparticles and the total arsenic concentration in the treated lake water sample was reduced to less than 0.01 g/L, meeting the USEPA standard for arsenic in drinking water. Thus, the $\alpha$-$Fe_2O_3$ nanoparticles are effective in removing both As(III) and As(V) from the natural water without the pre-oxidation and/or the pH adjustment.

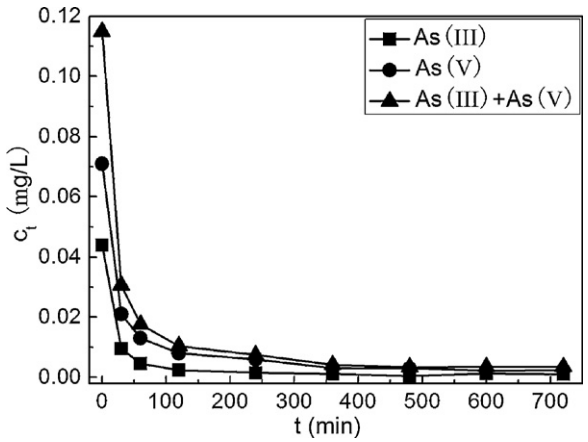


**Fig. 6.** The decrease of As(III) and As(V) concentration in a natural water sample from Lake Yangzonghai with the increase of the treatment time at a 0.1 g/L material loading of $\alpha$-$Fe_2O_3$.

## 4. Conclusions

Ultrafine $\alpha$-$Fe_2O_3$ nanoparticles were successfully synthesized by the solvent thermal process at low temperatures without the addition of surfactants or templates. These $\alpha$-$Fe_2O_3$ nanoparticles have a high specific surface area of ~162 $m^2$/g, and are rich in the surface hydroxyl groups. They demonstrated strong adsorption for As(III) and As(V) in the lab-prepared and natural water samples. The adsorption capacities of the $\alpha$-$Fe_2O_3$ nanoparticles for As(III) and As(V) were found to be over 95 mg/g and 47 mg/g, respectively, in the under neutral pH environment. The arsenic adsorption was particularly strong at very low arsenic concentrations and even in the presence of competing ions at very high concentrations. The high arsenic adsorption capacity at low equilibrium arsenic concentrations should benefit the applications of these adsorbents in real water environment where most contaminated water sources have relatively low arsenic concentrations. As these ultrafine $\alpha$-$Fe_2O_3$ nanoparticles could effectively remove most of arsenic contaminations (both As(III) and As(V)) from natural water samples of Lake Yangzonghai to meet the USEPA standard for arsenic in drinking water with only a relatively low material loading concentration (0.1 g/L), without the pre-oxidation and/or the pH adjustment, they may offer a simple single step treatment option to treat arsenic contaminated natural water effectively with relatively low cost and easy operation.

## Acknowledgments

This study was supported by the National Basic Research Program of China, Grant No. 2006CB601201, the Knowledge Innovation Program of Chinese Academy of Sciences, Grant No. Y0N5711171, and the Knowledge Innovation Program of Institute of Metal Research, Grant No. Y0N5A111A1.

## Appendix A. Supplementary data

Supplementary data associated with this article can be found, in the online version, at doi:10.1016/j.jhazmat.2011.04.111.

## References


[1] P. Mondal, C.B. Majumder, B. Mohanty, Laboratory based approaches for arsenic remediation from contaminated water: recent developments, J. Hazard. Mater. B 137 (2006) 464–479.
[2] B.K. Mandal, K.T. Suzuki, Arsenic round the world: a review, Talanta 58 (2002) 201–235.
[3] US EPA, Arsenic occurrence in public drinking water supplies, Washington, DC, 2000.
[4] D.N. Mazumder, N. Haque, B.K. Ghosh, A. De, D. Santra, A.H. Chakraborti, Arsenic in drinking water and the prevalence of respiratory effects in West Bengal India, Int. J. Epidemiol. 29 (6) (2000) 1047–1052.
[5] A.H. Smith, E.O. Lingas, M. Rahman, Contamination of drinking-water by arsenic in Bangladesh: a public health emergency, Bull. World Health Organ. 78 (9) (2000) 1093–1103.
[6] World Health Organization, Guidelines for drinking-water quality, health criteria and other supporting information, WHO, 2 (1996), pp. 940–949.
[7] D. Mohan, C.U. Pittman, Arsenic removal from water/wastewater using adsorbents—a critical review, J. Hazard. Mater. 142 (2007) 1–53.
[8] M. Vaclavikova, G.P. Gallios, S. Hredzak, S. Jakabsky, Removal of arsenic from water streams: an overview of available techniques, Clean Technol. Environ. Policy 10 (2008) 89–95.
[9] J.F. Ferguson, J. Gavis, Review of the arsenic cycle in natural waters, Water. Res. 6 (1972) 1259–1274.
[10] W.R. Penrose, Arsenic in the marine and aquatic environments; analysis, occurrence and significance, CRC Crit. Rev. Environ. Control 4 (1974) 465–482.
[11] M. Zaw, M.T. Emett, Arsenic removal from water using advanced oxidation processes, Toxicol. Lett. 133 (2002) 113–118.
[12] M.T. Uddin, M.S.I. Mozumder, M.A. Islam, S.A. Deowan, J. Hoinkis, Nanofiltration membrane process for the removal of arsenic from drinking water, Chem. Eng. Technol. 30 (9) (2007) 1248–1254.
[13] J.A. Saunders, M.K. Lee, M. Shamsudduha, P. Dhakal, Geochemistry and mineralogy of arsenic in (natural) anaerobic groundwaters, Appl. Geochem. 23 (2008) 3205–3214.
[14] T. Ashitani, T. Fujita, S. Katsuta, Composite Inorganic Oxide Adsorbent for Anions Removal from Polluted Water and its Preparation, Kokai Tokkyo Koho, Japan, 2000.
[15] D. Mishra, J. Farrell, Evaluation of mixed valent iron oxides as reactive adsorbents for arsenic removal, Environ. Sci. Technol. 39 (24) (2005) 9689–9694.
[16] V. Zaspalis, A. Pagana, S. Sklari, Arsenic removal from contaminated water by iron oxide sorbents and porous ceramic membranes, Desalination 217 (2007) 167–180.
[17] I. Balcu, A. Segneanu, M. Mirica, M. Iorga, C. Badea, I.F. Fitigau, Iron oxides from electrofilter ash for water treatment (arsenic removal), Environ. Eng. Manage. J. 8 (4) (2009) 895–900.
[18] S. Dixit, J.G. Hering, Comparison of arsenic(V) and arsenic(III) sorption onto iron oxide minerals: implications for arsenic mobility, Environ. Sci. Technol. 37 (2003) 4182–4189.
[19] H. Guo, D. Stuben, Z. Berner, Removal of arsenic from aqueous solution by natural siderite and hematite, Appl. Geochem. 22 (2007) 1039–1051.
[20] A.D. Redman, D.L. Macaldy, D. Ahmann, Natural organic matter affects arsenic speciation and sorption onto hematite, Environ. Sci. Technol. 36 (2002) 2889–2896.
[21] J. Giménez, M. Martínez, J.D. Pablo, M. Rovira, L. Duroc, Arsenic sorption onto natural hematite, magnetite, and goethite, J. Hazard. Mater. 141 (2007) 575–580.
[22] Y.M. Pajany, C. Hurel, N. Marmier, M. Romeó, Arsenic adsorption onto hematite and goethite, C.R. Chimie. 12 (2009) 876–881.
[23] H. Guo, D. Stuben, Z. Berner, U. Kramar, Adsorption of arsenic species from water using activated siderite–hematite column filters, J. Hazard. Mater. 151 (2008) 628–635.
[24] A. Redman, D. Macalady, D. Ahmann, Arsenic speciation and sorption onto hematite, Environ. Sci. Technol. 36 (2002) 2889–2896.
[25] I. Ko, J. Kim, K. Kim, Arsenic speciation and sorption kinetics in the As–hematite–humic acid system, Colloids Surf. A 234 (2004) 43–50.
[26] G. Ona-nguema, G. Morin, F. Juillot, G.E. Brown JR, EXAFS analysis of arsenite adsorption onto two-line ferrihydrite, hematite, goethite, and lepidocrocite, Environ. Sci. Technol. 39 (2005) 9147–9155.
[27] P. Sabbatini, F. Yrazu, F. Rossi, G. Thern, A. Marajofsky, M.M. Fidalgo de Cortalezzi, Fabrication and characterization of iron oxide ceramic membranes for arsenic removal, Water. Res. 44 (2010) 5702–5712.
[28] P. Sabbatini, F. Rossi, G. Thern, A. Marajofsky, Iron oxide adsorbers for arsenic removal: a low cost treatment for rural areas and mobile applications, Desalination 248 (2009) 184–192.
[29] K. Hristovski, A. Baumgardner, P. Westerhoff, Selecting metal oxide nanomaterials for arsenic removal in fixed bed columns: from nanopowders to aggregated nanoparticle media, J. Hazard. Mater. 147 (2007) 265–274.
[30] C.F. Cheng, W.Z. Zhou, D.H. Park, J. Klinowski, M. Hargreaves, L.F. Gladden, Controlling the channel diameter of the mesoporous molecular sieve MCM-41, J. Chem. Soc. Faraday Trans. 93 (1997) 359–363.
[31] H. Zhang, W.W. Wang, H.F. Li, S.L. Meng, D.Q. Li, A strategy to prepare ultrafine dispersed $Fe_2O_3$ nanoparticles, Mater. Lett. 62 (2008) 1230–1233.
[32] D.H. Chen, X.L. Jiao, D.R. Chen, Solvothermal synthesis of $\alpha$-$Fe_2O_3$ particles with different morphologies, Mater. Res. Bull. 36 (2001) 1057–1064.
[33] Z.H. Jing, S.H. Wua, S.M. Zhang, W.P. Huang, Hydrothermal fabrication of various morphological $\alpha$-$Fe_2O_3$ nanoparticles modified by surfactants, Mater. Res. Bull. 39 (2004) 2057–2064.
[34] Y.S. Ho, Ph.D. Thesis, University of Birmingham, Birmingham, UK, 1995.
[35] M.E. Pena, G.P. Korfiatis, M. Patel, L. Lippincott, X. Meng, Adsorption of As(V) and As(III) by nanocrystalline titanium dioxide, Water. Res. 39 (2005) 2327–2337.
[36] Y. Sag, Y. Aktay, Kinetic studies on sorption of Cr(VI) and Cu(II) ions by chitin, chitosan and rhizopus arrhizus, Biochem. Eng. J. 12 (2002) 143–153.
[37] K.P. Raven, A. Jain, R.H. Loeppert, Arsenite and arsenate adsorption on ferrihydrite: kinetics, equilibrium and adsorption envelopes, Environ. Sci. Technol. 32 (1998) 344–349.
[38] M.P. Yannick, C. Hurel, N. Marmier, M. Roméo, Arsenic adsorption onto hematite and goethite, C.R. Chimie. 12 (2009) 876–881.
[39] X.G. Meng, G.P. Korfiatis, S. Bang, K.W. Bang, Combined effects of anions on arsenic removal by iron hydroxides, Toxicol. Lett. 133 (2002) 103–111.
[40] X.H. Guan, H.R. Dong, J. Ma, L. Jiang, Removal of arsenic from water: effects of competing anions on As(III) removal in $KMnO_4$–Fe(II) process, Water Res. 43 (2009) 3891–3899.
[41] R.L. Parfitt, Anion adsorption by soil sand soil minerals, Adv. Agron. 30 (1978) 1–50.
[42] Y. Jeong, M.H. Fan, J.V. Leeuwen, J.F. Belczyk, Effect of competing solutes on arsenic(V) adsorption using iron and aluminum oxides, J. Environ. Sci. 19 (2007) 910–919.